Direct Strain Measurement of Polypyrrole Actuators Controlled by the Polymer/Gold Interface

Myoungho Pyo,[†,§] Clayton C. Bohn,[‡] Elisabeth Smela,[∥] John R. Reynolds,*[,†] and Anthony B. Brennan*[,‡]

Departments of Materials Science and Engineering and Chemistry, Center for Macromolecular Science and Engineering, University of Florida, Gainesville, Florida 32611-7200, Department of Chemistry, Sunchon National University, Sunchon, Chonnam 540-742, South Korea, and Department of Mechanical Engineering, University of Maryland, College Park, Maryland 20742

Received April 1, 2002. Revised Manuscript Received December 2, 2002

Electrochemically induced strain and actuation in a polypyrrole/Au/polyimide laminate was measured using a sensitive strain gage during oxidation and reduction (redox) of polypyrrole−ClO_4^-. The polyimide formed the top layer of the strain gage, allowing direct measurement of strain during redox switching in various electrolytes and potential windows. Strain increased in the order NaCl < $NaNO_3$ < $NaClO_4$. In the $NaClO_4$ solution for oxidizing potentials between 0.1 and 0.5 V vs Ag/AgCl, strain and charge were linearly proportional to voltage. Lower polypyrrole deposition potentials also increased strain. The surface roughness of the Au was varied by electrochemically depositing Au (which we designate EcAu) on top of thermally evaporated Au (EvAu)/polyimide. Greater EcAu deposition times led to greater Au roughness. Strain increased with polypyrrole thickness and Au roughness, which correlated with better adhesion between the polypyrrole and the Au. Au roughness also improved the cycling stability of the actuators.

Introduction

Conducting polymer actuators are candidates for various actuator applications, including robotics, microvalves, catheters, and antivibration systems.[1−10] Numerous studies have shown that the deposition of conducting polymers, such as polypyrrole (PPy), on mechanically inactive layers, such as metal/flexible plastic film bilayers, produces mechanical bending actuators.[6,11−23] The mechanism for the volume change is complex and involves the electrochemical transport of ions and solvent during redox cycling, along with other processes.[24−36] Most studies to date have indirectly determined in-plane strain from the curvature of bilayers of PPy[21−23,37−40] or have directly determined strain

* To whom correspondence should be addressed. E-mail: abren@mse.ufl.edu (A. B. Brennan); reynolds@chem.ufl.edu (J. R. Reynolds).
† Department of Chemistry, Center for Macromolecular Science and Engineering, University of Florida.
‡ Department of Materials Science and Engineering, Center for Macromolecular Science and Engineering, University of Florida.
§ Sunchon National University.
∥ University of Maryland.

(1) Irvin, D. J.; Goods, S. H.; Whinnery, L. L. *Chem. Mater.* **2001**, *13*, 1143.
(2) Tuijthof, G. J. M.; Herder, J. L. *Mech. Mach. Theory* **2000**, *35*, 945.
(3) Low, L. M.; Seetharaman, S.; He, K. Q.; Madou, M. J. *Sens. Actuators, B* **2000**, *67*, 149.
(4) Otero, T. F.; Grande, H.; Rodriguez, J. *Synth. Met.* **1996**, *76*, 293.
(5) Chen, X. W.; Xing, K. Z.; Inganas, O. *Chem. Mater.* **1996**, *8*, 2439.
(6) Kaneto, K.; Kaneko, M.; Min, Y.; MacDiarmid, A. G. *Synth. Met.* **1995**, *71*, 2211.
(7) Otero, T. F.; Grande, H.; Rodriguez, J. *J. Electroanal. Chem.* **1995**, *394*, 211.
(8) Baughman, R. H.; Shacklette, L. W.; Elsenbaumer, R. L.; Plichta, E. J.; Becht, C. Micro electromechanical actuators based on conducting polymers. In *Molecular Electronics*; Lazarev, P. I., Ed.; Kluwer Academic Publishers: Dordrecht, 1991; p 267.
(9) Baughman, R. H. *Synth. Met.* **1996**, *78*, 339.
(10) Della Santa, A.; De Rossi, D.; Mazzoldi, A.; Tiberi, M. Conducting polymer actuating structures for steerable microcatheters; Proceedings of the International Symposium on Microsystems, Intelligent Materials and Robots, Sendai, Japan, 1995.
(11) Otero, T. F.; Grande, H.-J. Electrochemomechanical Devices: Artificial Muscles Based on Conducting Polymers. In *Handbook of Conducting Polymers*, 2nd ed.; Skotheim, T. A., Elsenbaumer, R. L., Reynolds, J. R., Eds.; Marcel Dekker: New York, 1998; p 1015.
(12) Jager, E. W. H.; Smela, E.; Inganas, O. *Science* **2000**, *290*, 1540.
(13) Kaneko, M.; Kaneto, K. *React. Funct. Polym.* **1998**, *37*, 155.
(14) Lee, A. P.; Hong, K. C.; Trevino, J.; Northrup, M. A. Thin film conductive polymer for microactuator and micromuscle applications; Micro-Mechanical Systems Symposium of the International Mechanical Engineering Congress and Exposition, Chicago, IL, 1994.
(15) Lewis, T. W.; Spinks, G. M.; Wallace, G. G.; De Rossi, D.; Pachetti, M. *Polym. Prepr.* **1997**, *38*, 520.
(16) Madden, J. D.; Cush, R. A.; Kanigan, T. S.; Hunter, I. W. *Synth. Met.* **2000**, *113*, 185.
(17) Min, Y.; MacDiarmid, A. G.; Kaneto, K. *Polym. Mater. Sci. Eng.* **1994**, *71*, 713.
(18) Onoda, M.; Okamoto, T.; Tada, K.; Nakayama, H. *Jpn. J. Appl. Phys., Part 2* **1999**, *38*, L1070.
(19) Otero, T. F.; Angulo, E.; Rodriguez, J.; Santamaria, C. *J. Electroanal. Chem.* **1992**, *341*, 369.
(20) Otero, T. F. Artificial muscles, electrodissolution and redox processes in conducting polymers. In *Vol. 4. Conductive Polymers: Transport, Photophysics, and Applications*; Nalwa, H. S., Ed.; John Wiley & Sons: New York, 1997; p 517.
(21) Pei, Q. B.; Inganas, O. *J. Phys. Chem.* **1992**, *96*, 10507.
(22) Smela, E.; Inganas, O.; Lundstrom, I. *Science* **1995**, *268*, 1735.
(23) Pei, Q. B.; Inganas, O. *J. Phys. Chem.* **1993**, *97*, 6034.
(24) Pei, Q.; Inganas, O. *Synth. Met.* **1993**, *55−57*, 3718.
(25) Naoi, K.; Lien, M.; Smyrl, W. H. *J. Electrochem. Soc.* **1991**, *138*, 440.
(26) Gandhi, M. R.; Murray, P.; Spinks, G. M.; Wallace, G. G. *Synth. Met.* **1995**, *73*, 247.
(27) Chiarelli, P.; Dellasanta, A.; Derossi, D.; Mazzoldi, A. *J. Intell. Mater. Syst. Struct.* **1995**, *6*, 32.
(28) Torresi, R. M.; Detorresi, S. I. C.; Matencio, T.; Depaoli, M. A. *Synth. Met.* **1995**, *72*, 283.
(29) Yang, H.; Kwak, J. *J. Phys. Chem. B* **1997**, *101*, 774.

10.1021/cm020312w CCC: $25.00
Published on Web 02/01/2003

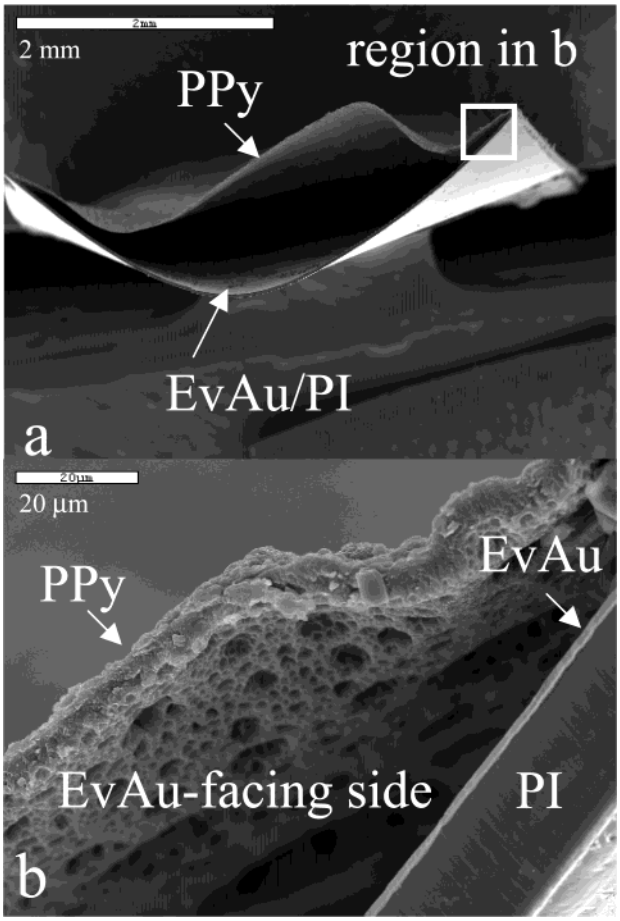

Figure 1. SEM micrograph of PPy delamination from EvAu.

by measuring length changes in conjugated polymer strips.[41,42] Out-of-plane strains have been measured using atomic force microscopy and have been found to be substantially larger than in-plane strains.[43]

A persistent problem with conjugated polymer/metal bilayers has been their short lifetime due to delamination of the polymer from the metal as a consequence of strain cycling. Repeated expansion and contraction of PPy causes the polymer to pull itself off the Au, which leads to reduced strain responses and eventual delamination as illustrated by Figure 1.

In this paper, we describe a new, quantitative way to measure in-plane strain, which results in bending, during redox switching of PPy deposited on a Au/polyimide (PI) strain gage (previously published as a brief communication[44]). This direct measurement of strain is made from resistance changes of a constantan grid that forms the sensing element of a commercially available strain gage that has been overcoated with Au and PPy layers. Here, we also report for the first time the use of rough, electrochemically deposited Au to increase the adhesion of PPy to the gold surface. We show the beneficial influence of Au roughness on strain and long-term stability.

Experimental Section

Chemicals. Pyrrole was vacuum-distilled and passed over neutral alumina until colorless before use. $NaClO_4$ and NaCl (Aldrich), $NaNO_3$ (Mallinckrodt Chemical Works), and Na_2SO_3 (Fisher Sci. Co.) were used as received. Electrochemical deposition of Au (EcAu) on thermally evaporated Au (EvAu) on polyimide (PI) utilized a commercial gold-plating solution of $Na_3Au(SO_3)_2$ (Oromerse SO Part B "Au replenisher") obtained from Technic Inc. For EcAu deposition, 10 mL of the solution was diluted by adding 30 mL of aqueous 1.7 M Na_2SO_3 as reported for electroless Au deposition.[45]

Strain Gages. Strain gages (CEA-06-500UW-120 and EA-06-20BW-120), consisting of a constantan foil grid sandwiched between two flexible PI layers, were purchased from Measurements Group, Inc. Such strain gages are capable of measuring strain with a precision of $\pm 1 \times 10^{-6}$ ϵ ($=\mu\epsilon$). The strain (ϵ) reported in this paper is defined as $\Delta L/L_0$, the change in the grid length (ΔL) relative to the length at a reference state (L_0). These devices have a strain limit of approximately $\pm 5\%$ (50 000 $\mu\epsilon$). The strain gages were connected to a strain indicator (P3500, Measurements Group, Inc.), which measured resistance changes in the strain gage.

Evaporated Au Films. Au was vacuum-deposited on one side of the PI surfaces by thermal evaporation (DV-502A, Denton Vacuum). Prior to deposition, 0.8 cm (w) $\times$ 5.3 cm (l) $\times$ 80 μm (t) strain gages, which had been stored in a 2-propanol solution, were washed with ethanol and double-distilled water successively. To reproducibly deposit EvAu layers, the vacuum was maintained below 10^{-3} Torr. No adhesive layer between EvAu and PI was used. The Au thickness, determined by scanning electron microscopy of a cross section of EvAu/PI, was $\approx$1.1 μm.

Electrochemically Deposited Au Films. All electrochemical work was carried out utilizing an EG&G Princeton Applied Research 273A potentiostat/galvanostat with a CorrWare software package. EvAu/PI gages were placed in a cell equipped with Pt counter and Ag/AgCl reference (BAS MF2052) electrodes. All potentials given in this paper are relative to this reference electrode. Electrical contact between the EvAu and the working electrode from the potentiostat was made using a conducting Cu tape (1181, 3M). EcAu layers were prepared potentiostatically on EvAu from the diluted Au solution mentioned above at -0.9 V.

The cathodic charge was varied to produce EcAu layers of different thicknesses, therefore yielding different surface roughness values. The surface topography of the Au was imaged using a scanning electron microscope (JEOL 6400). The surface roughness factor (γ) of the Au was determined from the ratio of the electrochemical area, obtained from the charge required to reduce the surface oxide layer,[46] to the geometric area. The electrochemical surface area of the Au was measured by potential cycling between 0.0 and 1.5 V in aqueous 50 mM H_2SO_4 solution. The charge during reoxidation of the gold oxide

(30) Yang, H.; Kwak, J. *J. Phys. Chem. B* **1997**, *101*, 4656.
(31) Yang, H.; Kwak, J. *J. Phys. Chem. B* **1998**, *102*, 1982.
(32) Peres, R. C. D.; Depaoli, M. A.; Torresi, R. M. *Synth. Met.* **1992**, *48*, 259.
(33) Maia, G.; Torresi, R. M.; Ticianelli, E. A.; Nart, F. C. *J. Phys. Chem.* **1996**, *100*, 15910.
(34) Slama, M.; Tanguy, J. *Synth. Met.* **1989**, *28*, C171.
(35) Song, M. K.; Gong, M. S.; Rhee, H. W. *Mol. Cryst. Liquid Cryst. Sci. Technol. Sect. A* **1996**, *280*, 145.
(36) Bay, L.; Jacobsen, T.; Skaarup, S.; West, K. *J. Phys. Chem. B* **2001**, *105*, 8492.
(37) Jager, E. W. H.; Inganas, O.; Lundstrom, I. *Adv. Mater.* **2001**, *13*, 76.
(38) Jager, E. W. H.; Smela, E.; Inganas, O.; Lundstrom, I. *Synth. Met.* **1999**, *102*, 1309.
(39) Jager, E. W. H.; Smela, E.; Inganas, O. *Sens. Actuators, B* **1999**, *56*, 73.
(40) Otero, T. F.; Sansinena, J. M. *Adv. Mater.* **1998**, *10*, 491.
(41) Della Santa, A.; De Rossi, D.; Mazzoldi, A. *Synth. Met.* **1997**, *90*, 93.
(42) Chiarelli, P.; Derossi, D.; Dellasanta, A.; Mazzoldi, A. *Polym. Gels Networks* **1994**, *2*, 289.
(43) Smela, E.; Gadegaard, N. *Adv. Mater.* **1999**, *11*, 953.
(44) Bohn, C. C.; Sadki, S.; Brennan, A. B.; Reynolds, J. R. *J. Electrochem. Soc.* **2002**, *149*, E281.
(45) Kang, M. S.; Martin, C. R. *Langmuir* **2001**, *17*, 2753.
(46) Gileadi, E.; Eisner, K. E.; Penciner, J. *Interfacial Electrochemistry. An Experimental Approach*; Addison-Wesley: Reading, MA, 1975.

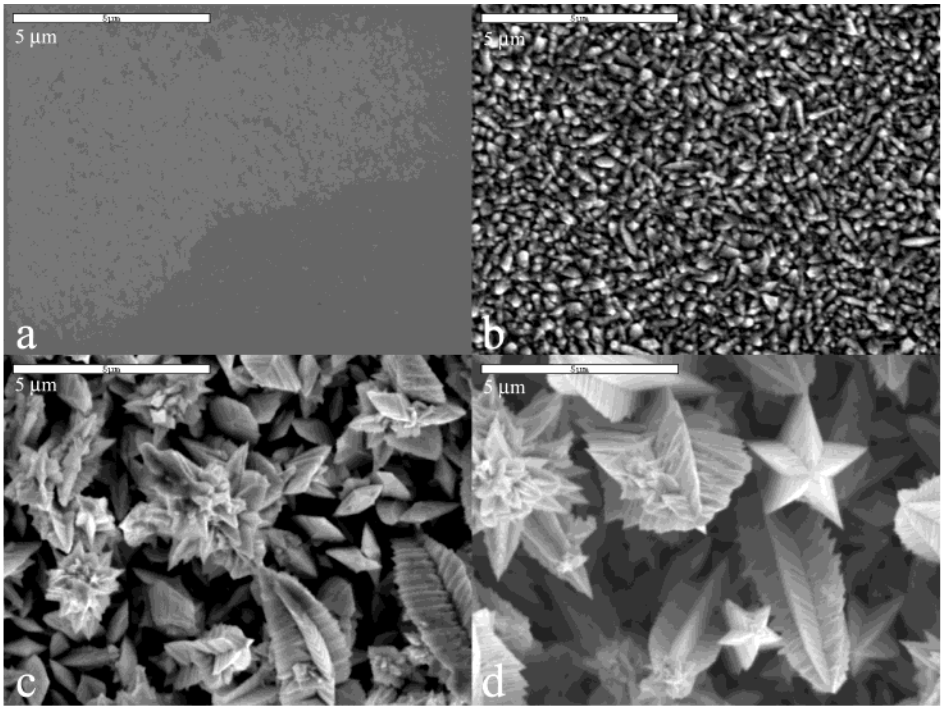

Figure 2. SEM micrographs for (a) EvAu ($\gamma = 2.89$) and EcAu surfaces after cathodic deposition of (b) 0.71 C cm^{-2} ($\gamma = 10.0$), (c) 2.36 C cm^{-2} ($\gamma = 18.9$), and (d) 4.72 C cm^{-2} ($\gamma = 24.5$). Scale bars are 5-μm long.

monolayer was converted to the surface area using a factor of 0.43 mC cm^{-2}.

Numerous studies on the electrodeposition of Au show that a variety of parameters, including electrolyte type, solution pH, additives, potentials, substrate structure, and so forth, affect the surface morphology of Au.[47−51] The morphological differences between the cathodically deposited Au and the EvAu are evident in the scanning electron microscopy (SEM) micrographs for different deposition charges shown in Figure 2. The relative smoothness of the EvAu, with a surface roughness factor $\gamma = 2.89$, is evident in Figure 2a. EcAu deposition at 0.71 C cm^{-2} ($\gamma = 10.0$) resulted in small crystals (Figure 2b). As the deposition charge increased, the crystals coalesced to form larger rodlike crystals in the shape of five-pointed Texas stars. These crystals continued to grow and coalesce to form larger stars, which were 2−3 μm in size after 4.72 C cm^{-2} ($\gamma = 24.5$). This topography is quite different than those of Au surfaces deposited chemically from a similar solution.[52,53]

Figure 3 illustrates that the surface roughness factor (γ) increased with EcAu deposition charge. The EcAu layer thickness also increased, which was measured using SEM micrographs of cross sections (Figure 4a). This suggests that growth of the Au crystals was predominantly perpendicular to the plane of the substrate.

PPy Films. PPy films of various thicknesses were synthesized potentiostatically on EcAu or EvAu from 0.1 M pyrrole in 0.1 M aqueous electrolytes at +0.9 V, unless otherwise mentioned. For most studies, the films were deposited from $NaClO_4$. Due to the roughness of the EcAu surface, direct determination of PPy film thickness on these surfaces was difficult (see Figure 4b). The charge passed during electropolymerization was therefore utilized to compare the effect of the amount of PPy on strain response. The polymerization charge ranged from 0.35 to 5.42 C cm^{-2}, which correlates with PPy film thicknesses of 1.25−19.4 μm on a smooth substrate, assuming 100% efficiency for the anodic deposition reaction and a charge−thickness ratio of 0.28 C μm^{-1} cm^{-2}.[54] The PPy films were then thoroughly washed with double-distilled water and the electrolyte solution used for the redox switching experiment. A 0.1 M $NaClO_4$ electrolyte was used unless otherwise mentioned.

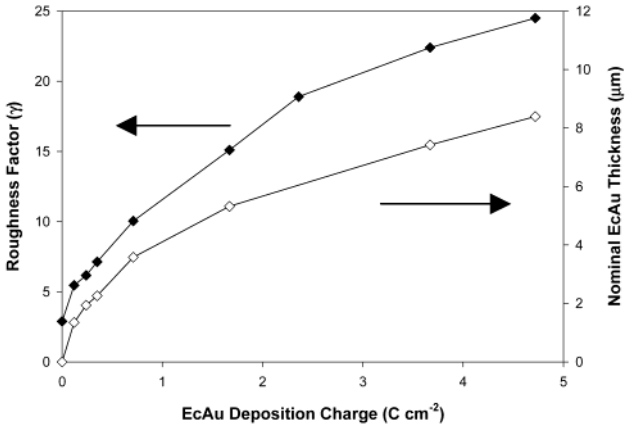

Figure 3. Change of roughness factor and EcAu thickness with EcAu deposition charge. EcAu thickness was determined from cross-sectional SEM micrographs.

Adhesion of PPy to the substrate was examined by a Scotch Magic tape (810, 3M) peel-off test. PPy (0.30 C cm^{-2}) was deposited on EvAu and EcAu surfaces and rinsed with distilled water. After drying in air for at least 24 h, the tape was placed on PPy and rubbed firmly using a fingernail. The tape was

(47) Finot, M. O.; Braybrook, G. D.; McDermott, M. T. *J. Electroanal. Chem.* **1999**, *466*, 234.
(48) Martin, H.; Carro, P.; Creus, A. H.; Gonzalez, S.; Salvarezza, R. C.; Arvia, A. J. *Langmuir* **1997**, *13*, 100.
(49) Schmidt, U.; Donten, M.; Osteryoung, J. G. *J. Electrochem. Soc.* **1997**, *144*, 2013.
(50) Li, Y. G.; Chrzanowski, W.; Lasia, A. *J. Appl. Electrochem.* **1996**, *26*, 843.
(51) Holmbom, G.; Jacobson, B. E. *J. Electrochem. Soc.* **1988**, *135*, 2720.
(52) Hou, Z. Z.; Dante, S.; Abbott, N. L.; Stroeve, P. *Langmuir* **1999**, *15*, 3011.
(53) Hou, Z. Z.; Abbott, N. L.; Stroeve, P. *Langmuir* **1998**, *14*, 3287.
(54) Zalewska, T.; Lisowska-Oleksiak, A.; Biallozor, S.; Jasulaitiene, V. *Electrochim. Acta* **2000**, *45*, 4031.

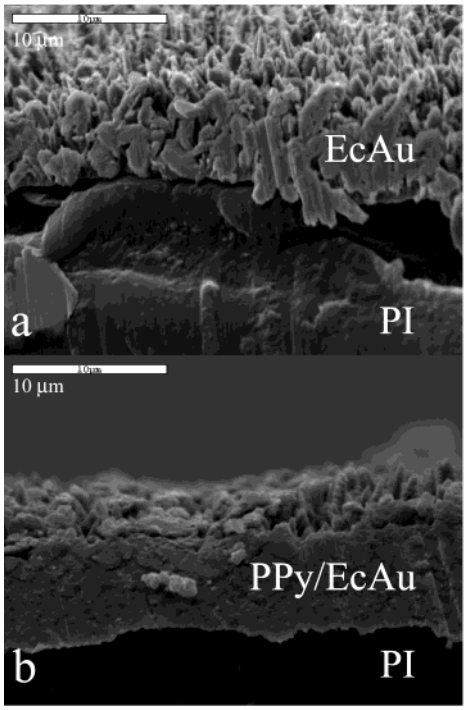

Figure 4. Cross-sectional SEM micrographs of (a) EcAu (γ = 18.9) and (b) PPy (18.9 C cm^{-2}) deposited on EcAu (γ = 18.9).

then removed slowly at a 90° angle with respect to the PPy surface.

Results and Discussion

Part 1. PPy/EvAu/Polyimide Actuators. We begin by discussing strain measurements of PPy films deposited on evaporated Au films. We examined the effects of electrolyte anion, potential limits during electrochemical stepping, and polymerization potential. In all of these experiments, a PPy polymerization charge of 2.83 C cm^{-2} was used, corresponding to an approximate thickness of 10 μm.

Effect of Anion during Electrochemical Cycling. It is well-known that the identity of the ionic and solvent species affects the actuation behavior of conducting and electroactive polymers.[9,23,25,55,56] We investigated the effect of anionic species on the strain response to confirm if the response could be correlated to the volume of solvated anions.

Figure 5 shows the strain responses of a ClO_4^--doped PPy/EvAu/PI actuator during potential cycling in ClO_4^-, NO_3^-, and Cl^- electrolyte solutions. After fully reducing the PPy at −0.6 V for 60 s, the potential was scanned at 5 mV s^{-1} to +0.4 V and then back to −0.6 V. The results were confirmed with two additional ClO_4^--doped samples and one NO_3^--doped sample; these PPy films were cycled with the other dopants in the same manner. These additional samples were run in a random order.

When cycled in $NaClO_4$, the actuator began to move in the plane at ca. −0.1 V (determined visually), which corresponded to the onset of the strain gage response (Figure 5a). The strain continued to increase due to PPy expansion and reached a maximum of 147 $\mu\epsilon$ during the reverse scan at ca. +0.3 V. Only a small difference in curvature was seen by eye between the reduced and oxidized states of the PPy, demonstrating the sensitivity and usefulness of the strain gage measurement. The detection of the maximum strain during the reverse scan indicates a slow expansion process of PPy relative to the time scale of this experiment. On the reverse scan, the strain decreased until it reached a minimum at −0.4 V.

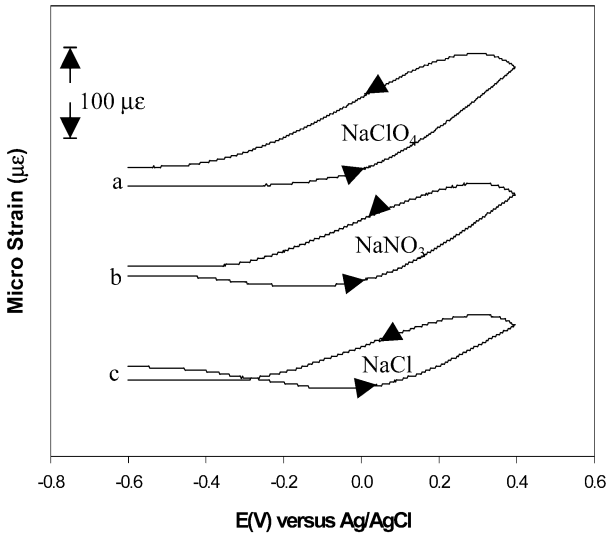

Figure 5. Strain responses of a PPy (2.83 C cm^{-2})/EvAu/PI actuator during potential cycling at 5 mV s^{-1} in (a) $NaClO_4$, (b) $NaNO_3$, and (c) NaCl aqueous solutions. Curves are offset for clarity.

After thorough washing, the actuator was immediately immersed in $NaNO_3$, and the potential was cycled 5 times to obtain reproducible strain responses. The maximum strain again occurred at ca. +0.3 V (Figure 5b), but was smaller than that of the actuator in $NaClO_4$, only 103 $\mu\epsilon$, which can be attributed to the smaller counterion. Moreover, a slight strain decrease was observed between −0.5 and −0.2 V during the initial portion of the forward scan. This is indicative of cation influx during reduction[24−26,32,33,35] and has also been shown by De Rossi and co-workers.[41] With the actuator in NaCl (Figure 5c), the maximum strain was again at ca. +0.3 V during the reverse scan, but reached only 57 $\mu\epsilon$. An initial decrease in strain, even more distinct than that of the actuator in $NaNO_3$, was again evident. Kaneto and co-workers have observed similar behaviors for poly(styrene sulfonate)-doped PPy.[57] They found that strain increase during PPy oxidation due to anion incorporation was linearly proportional to anion volume. A film cycled in $NaClO_4$ showed ca. 1.8 times higher strain response than that of the film in NaCl. Considering the solvated ionic volumes of Cl^- and ClO_4^- of 25 and 56 Å^3, respectively,[58] our result of 2.6 times higher strain in $NaClO_4$ also indicates that ion exchange during redox switching of PPy is the dominant mechanism for strain changes.

Effect of Potential Limits. Utilizing the strain gage methodology, the influence of the doping level was

(55) Skaarup, S.; West, K.; Gunaratne, L.; Vidanapathirana, K. P.; Careem, M. A. *Solid State Ionics* **2000**, *136*, 577.
(56) Reynolds, J. R.; Pyo, M.; Qiu, Y. J. *Synth. Met.* **1993**, *55*, 1388.
(57) Sonoda, Y.; Takashima, W.; Kaneto, K. *Synth. Met.* **2001**, *119*, 267.
(58) Kaneko, M.; Fukui, M.; Takashima, W.; Kaneto, K. *Synth. Met.* **1997**, *84*, 795.

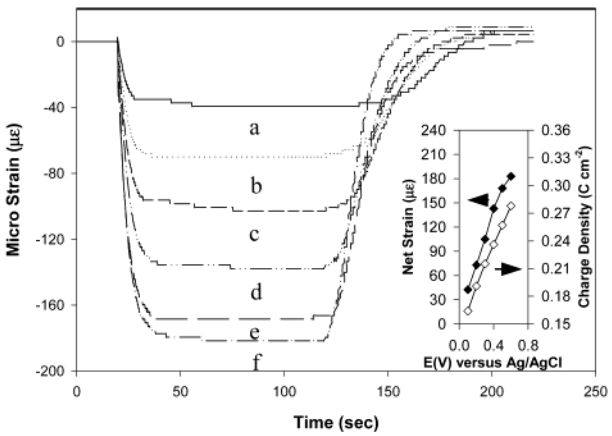

Figure 6. Strain responses of a PPy (2.83 C cm^{-2})/EvAu/PI actuator during potential stepping in $NaClO_4$ between −0.6 and (a) +0.1 V, (b) +0.2 V, (c) +0.3 V, (d) +0.4 V, (e) +0.5 V, and (f) +0.6 V. The films were oxidized and reduced for 100 seconds each; the plot shows half a reduction step before and after the oxidation step.

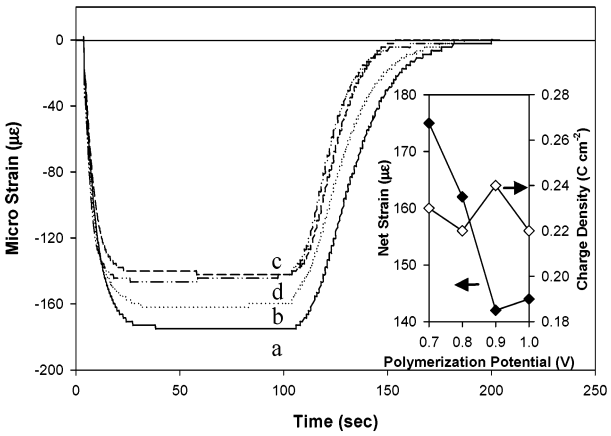

Figure 7. Strain responses of a PPy (2.83 C cm^{-2})/EvAu/PI actuator during potential stepping in $NaClO_4$ between −0.6 and +0.4 V. PPy was potentiostatically prepared at (a) +0.7 V, (b) +0.8 V, (c) +0.9 V, and (d) +1.0 V. Inset shows the maximal strain and charge changes during PPy oxidation.

investigated by stepping the applied potential in $NaClO_4$. This was done to determine whether there was a discrepancy between the consumed charge and the strain. Two runs were done at each potential on the same sample, and the order of the potentials was randomized. The PPy was oxidized at potentials of +0.1 to +0.6 V, reduced at −0.6 V, and again oxidized at the initial potential. The strain responses were normalized for comparison of the overall change in strain. Figure 6 shows that the magnitude of the normalized strain response depended almost linearly on the original oxidizing potential within this voltage range, as did the consumed charge. This confirms that the number of anions in the film, which can be controlled by the doping level of the PPy, is the dominant factor determining the strain.[59] The oxidation process was somewhat slower than the reduction process, especially for the smaller potential steps from 0.1 and 0.2 V.

Effect of Polymerization Potential. To help determine optimal preparation conditions for this material, the influence of polymerization potential on actuation properties was investigated. Recently, Maw et al.[60] demonstrated that for PPy(dodecylbenzenesulfonate)/Au/Kapton laminates prepared galvanostatically in aqueous solutions, bending was greater for low deposition current densities (0.4 mA/cm^2) than for high deposition current densities (40 mA/cm^2).

In this work, strain in $NaClO_4$ also correlated inversely with polymerization rates (Figure 7). The strain for PPy (2.83 C cm^{-2}) actuators prepared potentiostatically at either +0.9 or +1.0 V was smaller by 20% compared to those prepared at +0.7 V; this was also confirmed later in the EcAu actuators. This result is not due to a decrease in the electroactivity of PPy: the strain differential shown in the inset to Figure 7 shows that each film had similar switching charge densities during PPy oxidation. We find the polymerization potential of +0.7 V to be optimum in this case for a maximum strain response. It is possible that the higher polymerization potentials yield a higher degree of cross-linking (a tighter network), and thus the ability of the polymer to strain is reduced.

Part 2. PPy/EcAu/EvAu/Polyimide Actuators. In this section, we describe results obtained with electrochemically deposited Au films. We compare EvAu and EcAu substrates with respect to adhesion, strain, frequency response, and long-term cycling. Unless otherwise specified, PPy films were used and the electrolyte was $NaClO_4$.

Adhesion. The adhesion of PPy films to EcAu and EvAu was tested by a tape peel-off test. The PPy films were deposited, rinsed, dried in air for at least 24 h, and subsequently tested. Three PPy films deposited on EvAu were readily removed. PPy on EcAu ($\gamma \geq 10$), on the other hand, exhibited excellent adhesion with no evidence of delamination for 11 samples. We attribute the significantly enhanced adhesion between PPy and the substrate to the "nooks and crannies" created by the EcAu deposition, within which the PPy is mechanically interlocked (see Figure 4b).

Strain. Three PPy (1.18 C cm^{-2}) samples were deposited on EvAu with $\gamma = 2.89$ and EcAu with $\gamma =$ 6.17, 7.13, 10.0, 18.9, and 24.5. They were evaluated by potential stepping between −0.6 and +0.4 V. The strains for various γ values are shown in Figure 8. Increasing the roughness increased the strain up to $\gamma = 10$ and then decreased it for $\gamma = 18.9$ and 25. This increase and then decrease in strain is due to the relative thicknesses of the EcAu and PPy layers. As the surface roughness increases, the surface area also increases, therefore decreasing the PPy film thickness (for a given polymerization charge). When the EcAu thickness exceeds the PPy thickness, it is harder for the PPy to bend the EcAu layer; therefore, a decrease in the strain response is recorded.

In an independent set of experiments in which each point was duplicated, strain vs amount of PPy was examined. Strain rose with an increasing amount of PPy deposited for all values of γ (Figure 9). This was expected from basic mechanics. For a polymerization charge of 1.18 C/cm^2, the maximum strain increased up to $\gamma = 10$ and then decreased again, as in Figure 8. Curves D and E in Figure 9 show that as the thickness

(59) Otero, T. F.; Sansiñena, J. M. *Bioelectrochem. Bioenerg.* **1997**, *42*, 117.

(60) Maw, S.; Smela, E.; Yoshida, K.; Sommer-Larsen, P.; Stein, R. B. *Sens. Actuators, A* **2001**, *89*, 175.

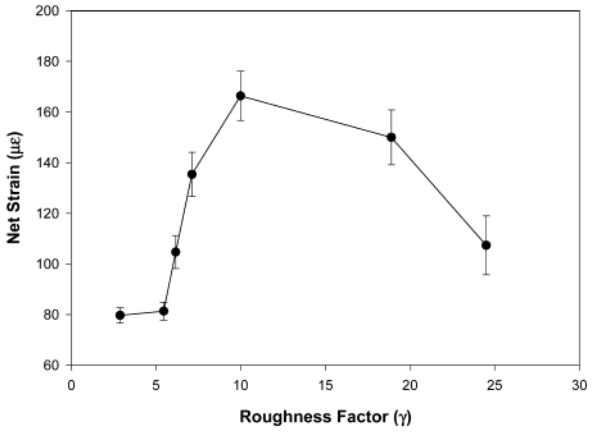

Figure 8. Strain change as a function of roughness factor γ during potential stepping between −0.6 and +0.4 V. PPy (1.18 C cm^{-2}) was deposited on EvAu with $\gamma = 2.89$ and EcAu with $\gamma = 6.17$, 7.13, 10.0, 18.9, and 24.5.

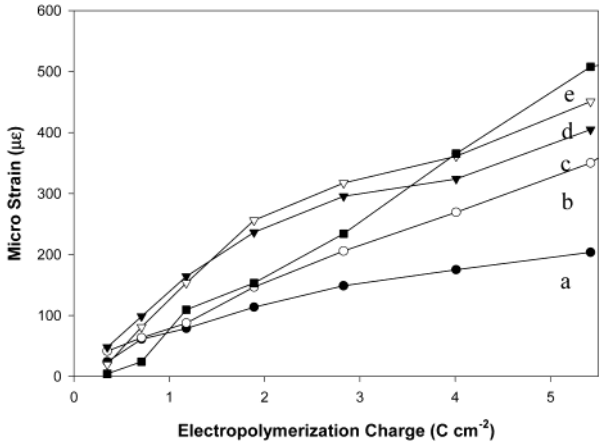

Figure 9. Maximum strain changes during potential stepping between −0.6 and +0.4 V with increasing electropolymerization charges of pyrrole on (a) EvAu ($\gamma = 2.89$) and EcAu of γ = (b) 6.17, (c) 10.0, (d) 18.9, and (e) 24.5.

of the PPy increased, the optimal γ shifted to larger values. This result indicates that surface roughness and the amount of PPy deposited simultaneously affect bending. Again, this was as expected: as the thickness of the PPy increases, the optimal thickness for the substrate also increases to obtain a minimal bending radius.

Frequency Response. One actuator each of PPy(1.18 C cm^{-2})/EvAu(γ=2.89) and PPy(1.18 C cm^{-2})/EcAu(γ=10.0) were stepped between −0.6 and +0.4 V at increasing frequencies (0.01−0.5 Hz). Although strain and charge decreased as a function of increasing frequency, the strains for the PPy/EcAu were greater than those for the PPy/EvAu at all frequencies (see Figure 10).

Whereas the charge exchanged during oxidation and reduction also decreased with increasing switching frequency (Figure 10), the PPy/EcAu had a higher strain per unit charge (inset Figure 10). This greater efficiency might be either a result of stronger adhesion of PPy to the substrate or smaller ohmic drops in the PPy because of shorter distances to the electrode. The EcAu is thus also beneficial to actuator efficiency.

Long-Term Cycling. PPy with an electropolymerization charge of 1.18 C cm^{-2} was subjected to multiple

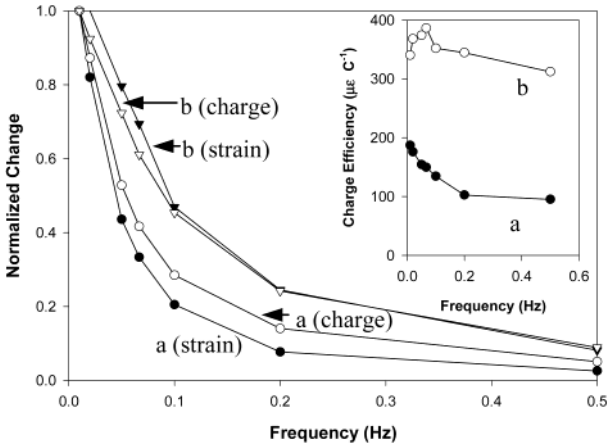

Figure 10. Normalized strain and charge responses of PPy (1.18 C cm^{-2}) on (a) EvAu ($\gamma = 2.89$) and (b) EcAu ($\gamma = 10.0$) relative to values at 0.01 Hz. Inset shows the ratios of the strain to the charge as a function of the frequency.

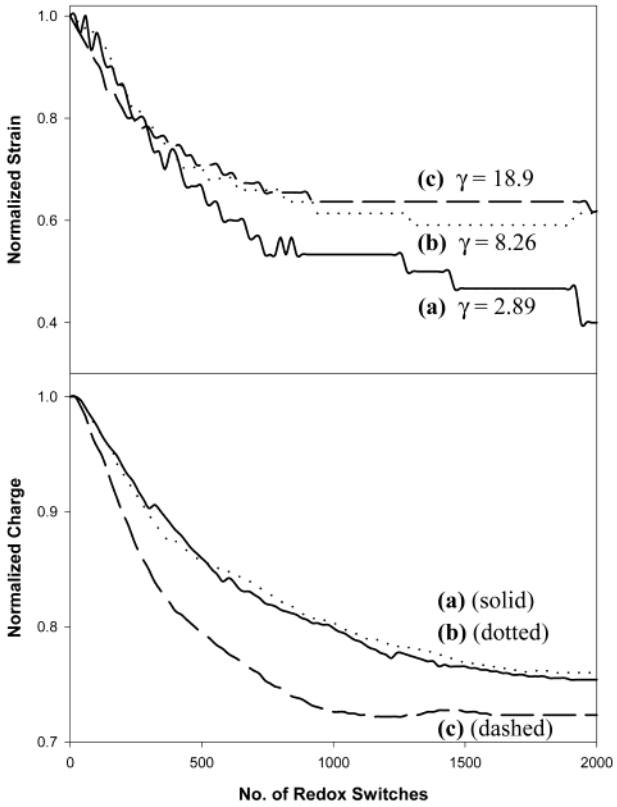

Figure 11. Strain and charge of PPy (1.18 C cm^{-2}) on (a) EvAu ($\gamma = 2.89$), (b) EcAu ($\gamma = 8.26$), and (c) EcAu ($\gamma = 18.9$) with repeated potential switches between −0.6 V for 10 s and +0.4 V for 20 s.

potential steps of reduction at −0.6 V for 10 s and oxidation at +0.4 V for 20 s. Two samples each of PPy on EvAu ($\gamma = 2.89$) and EcAu (with $\gamma = 8.26$ and 18.9) were examined for 2000 cycles, and the results are presented in Figure 11. PPy/EcAu has improved long-term switching stability compared with PPy/EvAu. The strain continually decreased with the number of redox switches in curve a, but the strain in curves b and c stabilized after 1000 switches, retaining 60% of the initial strain. The magnitude of the consumed charge decrease was smaller, dropping in all three cases to ∼75% of the original value. This result implies that the

long-term stability of the strain is improved by utilizing the EcAu deposition method, helping to solve the delamination problem. It also shows that the strain does not always correlate directly to the amount of charge exchanged during PPy redox alone, but must include the mechanical coupling between PPy and the substrate.

Conclusions

The strain of PPy/Au/PI bending actuators during redox switching of PPy was directly and quantitatively monitored using an in situ strain gage, a sensitive and reliable method. The results support previously reported trends for the effect of deposition potentials and redox switching of PPy.

The roughness of the substrate significantly affects the maximum strain attainable. When the surface roughness and the amount of PPy are judiciously chosen, the actuator exhibits 3 times higher strain than PPy actuators prepared with a thermally evaporated Au surface. It is also important that long-term stability is significantly improved by good adhesion between PPy and the EcAu. These effects are probably a result of better adhesion and electrical contact due to mechanical interlocking of the PPy and the metal electrode.

Acknowledgment. We appreciate funding of this work through the DARPA/ARO Grant DAAD19-00-1-0002.

CM020312W